

12

AD-A161 826

AD



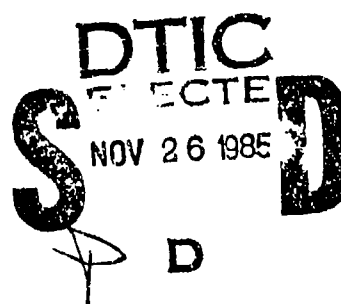
US ARMY  
MATERIEL  
COMMAND

TECHNICAL REPORT BRL-TR-2685

A STUDY ON THE EFFECTS OF VARIABLE  
SURFACE AREA TO VOLUME RATIO ON  
CLOSED BOMB BURN RATES

Robert E. Tompkins  
Roger E. Bowman  
Arpad A. Juhasz

October 1985



APPROVED FOR PUBLIC RELEASE; DISTRIBUTION UNLIMITED.

US ARMY BALLISTIC RESEARCH LABORATORY  
ABERDEEN PROVING GROUND, MARYLAND

DTIC FILE COPY

85 11 25 021

Destroy this report when it is no longer needed.  
Do not return it to the originator.

Secondary distribution of this report is prohibited.

Additional copies of this report may be obtained  
from the Defense Technical Information Center,  
Cameron Station, Alexandria, Virginia 22314.

The findings in this report are not to be construed as  
an official Department of the Army position, unless so  
designated by other authorized documents.

The use of trade names or manufacturers' names in this report  
does not constitute indorsement of any commercial product.

UNCLASSIFIED

SECURITY CLASSIFICATION OF THIS PAGE (When Data Entered)

REPORT DOCUMENTATION PAGE		READ INSTRUCTIONS BEFORE COMPLETING FORM
1. REPORT NUMBER	2. GOVT ACCESSION NO.	3. REPORT CATALOG NUMBER
Technical Report BRL-TR-2685	AD-A161826	
4. TITLE (and Subtitle) A Study on the Effects of Variable Surface Area to Volume Ratio on Closed Bomb Burn Rates		5. TYPE OF REPORT & PERIOD COVERED Final
6. AUTHOR(s) R.E. Tompkins, R.E. Bowman,* and A.A. Juhasz		7. PERFORMING ORG. REPORT NUMBER
8. PERFORMING ORGANIZATION NAME AND ADDRESS US Army Ballistic Research Laboratory ATTN: SLCBR-IB Aberdeen Proving Ground, MD 21005-5066		9. CONTRACT OR GRANT NUMBER(s)
10. CONTROLLING OFFICE NAME AND ADDRESS US Army Ballistic Research Laboratory ATTN: SLCBR-DD-T Aberdeen Proving Ground, MD 21005-5066		11. PROGRAM ELEMENT, PROJECT, TASK AREA & WORK UNIT NUMBER
12. MONITORING AGENCY NAME & ADDRESS (if different from Controlling Office)		13. REPORT DATE October 1985
		14. NUMBER OF PAGES 43
		15. SECURITY CLASS. (of this report) Unclassified
		16. DECLASSIFICATION/DOWNGRADING SCHEDULE
17. DISTRIBUTION STATEMENT (of this Report) Approved for public release; distribution unlimited.		
18. DISTRIBUTION STATEMENT (of the abstract entered in Block 20, if different from Report)		
19. SUPPLEMENTARY NOTES *Retired		
20. KEY WORDS (Continue on reverse side if necessary and identify by block number) Burning Rate Closed Bomb Heat Loss		
21. ABSTRACT (Continue on reverse side if necessary and identify by block number) In response to various discussions on the effects of heat loss on propellant burn rates, an experimental matrix was set up to systematically examine the effects of surface area to volume ratio and loading density on derived burn rates. The propellant used in this study was single perforated M-10 with a web of .058 cm. The surface area to volume ratios (s/v) used were 1, 2, 3, and 5/cm <sup>2</sup> . The loading densities varied from 0.1 to 0.4 g/cc.		

DD FORM 1 JAN 73 1473

EDITION OF 1 NOV 65 IS OBSOLETE

UNCLASSIFIED

SECURITY CLASSIFICATION OF THIS PAGE (When Data Entered)

CP Sub may

UNCLASSIFIED

SECURITY CLASSIFICATION OF THIS PAGE(When Data Entered)

20. ABSTRACT (Cont)

The resultant pressure-time data showed a reduction in maximum pressure ( $P_{max}$ ) at constant loading density as the s/v increased. This data was reduced via CBRED2, our closed bomb burning rate reduction program. Burning rate reproducibility was excellent from run to run. There was very good agreement in the derived burn rates for the 0.2, 0.3, and 0.4 g/cc loading densities. Using the constant heat loss option, the variations in s/v had little or no effect on derived burning rates from 30% to 90% of  $P_{max}$ . At less than 30%  $P_{max}$ , there seemed to be no consistent effect on the burn rates from varying the s/v. When data was reduced using the proportional heat loss option, burning rates, as well as their slopes, tended to increase as the s/v increased. Considering the extreme variations in the surface area available for heat loss in the experiments, burning rates do not appear to be very sensitive to large s/v changes.

UNCLASSIFIED

SECURITY CLASSIFICATION OF THIS PAGE(When Data Entered)

11

# TABLE OF CONTENTS

	<u>Page</u>
LIST OF ILLUSTRATIONS.....	5
I. INTRODUCTION.....	7
II. EXPERIMENTAL.....	9
III. RESULTS & DISCUSSION.....	12
IV. CONCLUSIONS & RECOMMENDATIONS.....	23
ACKNOWLEDGEMENTS.....	24
REFERENCES.....	25
APPENDIX .....	27
DISTRIBUTION LIST.....	35

Accession For	
NTIS CRA&I	<input checked="checked" type="checkbox"/>
DTIC TAB	<input type="checkbox"/>
Unannounced	<input type="checkbox"/>
Justification .....	
By .....	
Distribution/ .....	
Availability Codes	
Dist	Avail and/or Special
<b>A-1</b>	



# LIST OF ILLUSTRATIONS

Figure	Page
1 High Pressure Closed Chamber Used for Propellant Testing.....	10
2 Typical Charge Configuration With Coil Assembly.....	11
3 Overplots Showing Constant Loading Density at 0.3 g/cc with s/v of 1, 2, 3, & 5 cm <sup>-1</sup> . All Data Reduced Using the Constant Heat Loss Option.....	14
4 Overplots Showing Constant s/v of 3 cm <sup>-1</sup> with Loading Densities at 0.1, 0.2, 0.3, & 0.4 g/cc. All Data Reduced Using the Constant Heat Loss Option.....	16
5 Overplots Showing Constant Loading Density at 0.4 g/cc with s/v of 1, 2, 3, & 5 cm <sup>-1</sup> . All Data Reduced Using the Proportional Heat Loss Option.....	17
6 Overplots Showing Constant s/v of 3 cm <sup>-1</sup> with Loading Densities at 0.1, 0.2, 0.3, & 0.4 g/cc. All Data Reduced Using the Proportional Heat Loss Option.....	18
7 Overplots Showing Constant Loading Density at 0.2 g/cc and Constant s/v of 1 cm <sup>-1</sup> . Data Reduced Using the Proportional (P), Constant (C), and Zero (0) Heat Loss Options.....	20
8 Overplots Showing Constant Loading Density at 0.2 g/cc and Constant s/v 5 cm <sup>-1</sup> . Data Reduced Using the Proportional (P), Constant (C), and Zero (0) Heat Loss Options..	21
A-1 Constant heat loss option. Superimposed plots of s/v ratio vs Burn Rate.....	29
A-2 Porportional heat loss option. Superimposed plots of s/v ratio vs Burn Rate.....	30
A-3 All heat loss options. Superimposed burning rate plots at 0.3 g/cc and s/v = 1 cm <sup>-1</sup> . Data reduced using; proportional heat loss option & tabular thermochems (PT), proportional heat loss option & average thermochems (PA), constant heat loss option & average thermochems (CA).....	31
A-4 All heat loss options. Superimposed burning rate plots at 0.3 g/cc and s/v = 5 cm <sup>-1</sup> . Data reduced using; proportional heat loss option & tabular thermochems (PT), proportional heat loss option & average thermochems (PA), constant heat loss option & average thermochems (CA).....	32
A-5 Proportional heat loss option & tabular thermochems. Superimposed burning rate plots at 0.3 g/cc with s/v = 1 cm <sup>-1</sup> (solid line) and 0.3 g/cc with s/v = 5 cm <sup>-1</sup> (dotted line).....	33

## I. INTRODUCTION

At the BRL, as in many other ballistic laboratories, closed bomb experiments are used to provide information on the burning characteristics of gun propellants. One significant advantage of the closed bomb technique is its ability to provide burning rate data over a wide pressure range from a limited number of experiments. A further advantage is that the combustion conditions in the closed bomb approximate the combustion conditions in the gun. Significantly, the bomb permits examination of propellants in the exact geometry and granulation as used in the gun. The principal disadvantage of the closed bomb method, however, is the complexity of the data reduction technique. Tied in with this is the necessity to make a variety of assumptions and simplifications during the theory development to make the treatment tractable, even when using a computer.

Early lumped parameter interior ballistic treatments viewed closed bomb propellant burning rate data as empirical information to be adjusted by the ballisticians, according to somewhat subjective criteria, to help obtain a suitable ballistic match between the measured gun firings and the code simulations. In effect, the doctored burning rates were used to help account for factors not explicitly treated in the interior ballistic models; factors such as erosive burning effects, bore friction, and heat loss.

In the 1970's, with the development of increasingly sophisticated interior ballistic codes which sought to include more of the physics involved in the interior ballistic event, a strong interest arose in burning rates as intrinsic propellant properties as opposed to empirical information. This interest spawned the development of a number of closed bomb burning rate codes incorporating, in their turn, a more exact treatment of the combustion process in the bomb. Notable among these were the works by Price<sup>1</sup>, Robbins<sup>2</sup> and Krier.<sup>3</sup> The development of the codes was, in turn, followed by comparison studies of the relative values of burning rates obtained from closed bombs and strand burners. Since strand burner measurements only involve the measurement of time for a given length of sample to burn at a fixed pressure, agreement between the two methods would constitute an excellent calibration of computed closed bomb burning rates

---

<sup>1</sup>C. Price and A. Juhasz, "Versatile User-Oriented Closed Bomb Data Reduction Program (CBRED)," Ballistic Research Laboratories Report, BRL Report No. 2018, September 1977.

<sup>2</sup>F.W. Robbins and A.W. Horst, "Numerical Simulation of Closed Bomb Performance Based on BLAKE Code Thermodynamic Data," Indian Head Memorandum Report, IHMR 76-259, November, 1976.

<sup>3</sup>H. Krier, "Extracting Burning Rates for Multiperforated Propellant From Closed Bomb Testing," Aeronautical and Astronautical Engineering Department, University of Illinois at Urbana-Champaign, Technical Report AAE 78-2, UIU-ENG 78-0502, July, 1978.

against measured quantities. At least two independent studies<sup>4 5</sup> confirmed the agreement between the methods. The comparability of closed bomb burning rate data (on identical propellant samples) from various US installations was examined under a JANNAF sponsored round robin study.<sup>5</sup> The agreement between installations was, ultimately, quite good. This indicated that the differences in computational methods were minor as far as the final results were concerned.

The results of the round robin study brought up the question as to the necessity of modeling heat loss to the bomb and if necessary, what kind of model should be used and how rigorous should it be treated. The various closed bomb codes used in the round robin for data reduction did use different heat loss treatments. The SIMPCB<sup>2</sup> code, which was used by Naval Ordnance Station for data reduction, has a heat loss treatment that derives a constant from the difference between the theoretical and the observed maximum pressure and multiplies that constant by various pressures to get the heat loss at that pressure. The Large Caliber Weapon Systems Laboratory at Dover reduced their data using NCBOMB, which models heat loss indirectly by using  $P/P_{\max}$  for burn rate. The Naval Weapons Center at China Lake uses a modified version of CBRED for data analysis. The CBRED2 code was used by the Ballistic Research Laboratory for the round robin study. This code has two heat loss options that include a constant averaging based on the difference between the observed pressure and the adiabatic prediction, and a proportional method derived from the post  $P_{\max}$   $dP/dt$  data. The constant averaging, or standard, option computes the total heat loss by taking the difference between the computed adiabatic internal energy of the system and the internal energy observed from  $P_{\max}$ . This is then divided by the total burn time to get an average heat loss rate. The proportional option analyzes the heat loss into its radiative and convective components. It is assumed that during the actual event, the heat loss is due to both convection and radiation to the chamber walls. The further assumption is that after burning has ceased, the entire heat loss is due to radiation alone. Using the ideal-gas law, a temperature-time profile of the post  $P_{\max}$  data is obtained. This is matched to a radiative heat loss rate calculated from the same  $dP/dt$  data. Now, this array along with the wall surface area is used to generate a radiative heat transfer coefficient that remains a constant throughout the analysis. Once the radiative heat transfer coefficient is known, this is used in conjunction with the mass generation rate to compute a convective heat transfer coefficient at every point in the analysis. The program now computes the heat loss rate for each data point using standard heat transfer techniques.

Locally, we became concerned when we noted significant discrepancies between closed bomb burning rates of identical propellants reduced using the

---

<sup>4</sup>S. Mitchell and A. Horst, "Comparative Burning Rate Study," CPIA Publication 281, Bulletin of the 13th JANNAF Combustion Meeting, Chemical Propulsion Information Agency, Johns Hopkins University/Applied Physics Laboratory, September, 1976.

<sup>5</sup>A.A. Juhasz, Ed., "Round Robin Results of the Closed Bomb and Strand Burner," Applied Physics Laboratory, CPIA Publication 361, July, 1982.



same reduction code, CBRED2. The difference in the data could be traced to the bombs in which the samples were fired. One of these was the standard 200 cc chamber used in the round robin study. The other was a fixture adapted from the breech section of a 0.50 caliber gun. A check on the ignition methods failed to account for the difference. An examination of the fixtures, however, revealed significant differences in the surface area to volume ratios (s/v) of the two devices ( $2.67 \text{ cm}^{-1}$  in the 0.50 cal. fixture and  $.924 \text{ cm}^{-1}$  in the 200 cc device) and in the thermal conductivities of the chamber walls. (The 0.50 cal. fixture used a brass cartridge case to contain the propellant while the walls of the 200 cc bomb were steel). The question came down to whether the differences noted in burning rates could be due to increased heat loss during burning as a result of the increased s/v and/or increased thermal conductivity of the brass case-lined 0.50 caliber fixture.

Coincidentally a series of experiments had been set up to confirm the accuracy of the BLAKE code. The experiment involved varying the s/v ratio of the closed bomb ( $1-5 \text{ cm}^{-1}$ ), by using steel coil inserts, for multiple loading densities ( $0.1-0.4 \text{ g/cc}$ ). The propellant was to be a fast burning, single base propellant. The decision was made to use the data from that series of closed bomb shots as a starting point and add some additional shots using a propellant with a slower burning rate while replacing the steel coils, used to vary s/v, with brass coils to round out the matrix.

## II. EXPERIMENTAL

Closed chamber tests were performed in the 850 MPa test fixture described in Fig. 1 and manufactured by Harwood Engineering. The chamber cavity was 10.9 cm long and 5.08 cm in diameter with a hemispherical rear inner surface. The volume used for data calculations was 210 cc. Pressure measurements were made with a Kistler 607C4 transducer tied into a Kistler 504E charge amplifier. Data acquisition was made on a Nicolet Explorer III digital oscilloscope, followed by data reduction on a PDP 11/34 computer using the CBRED2 code.

The surface area to volume ratios were adjusted by using steel or brass insert coils of varying diameters and nesting one inside the other when necessary. These ratios ranged from  $0.924 \text{ cm}^{-1}$  to  $5.05 \text{ cm}^{-1}$ . Fabrication of the coils was done on a mass basis by first determining the mass per unit length of the wire in use, calculating the volume that the coil was to occupy, wrapping the wire around a suitable mandrel, and trimming the resulting coil to obtain the correct mass.

Samples were ignited using an Atlas M-100 electric match with 1 g clean burning ignition material (CBI) enclosed in a dacron patch tied around the head of the match. CBI, rather than black powder, was used as the igniter material for more exact thermochemical calculations in the BLAKE code. The propellant used for most of the firings was M-10, Lot RAD-PE-481-27. A limited number of shots were fired using NOSOL 363, Lot RAD-1-1. The NOSOL 363 was fired with two separate web sizes, 0.271 cm and 0.031 cm. All of the samples were prepared immediately before firing according to our usual procedure in which the sample was bagged in a cellophane tube with the igniter in the front section of the charge (see Fig. 2). The samples

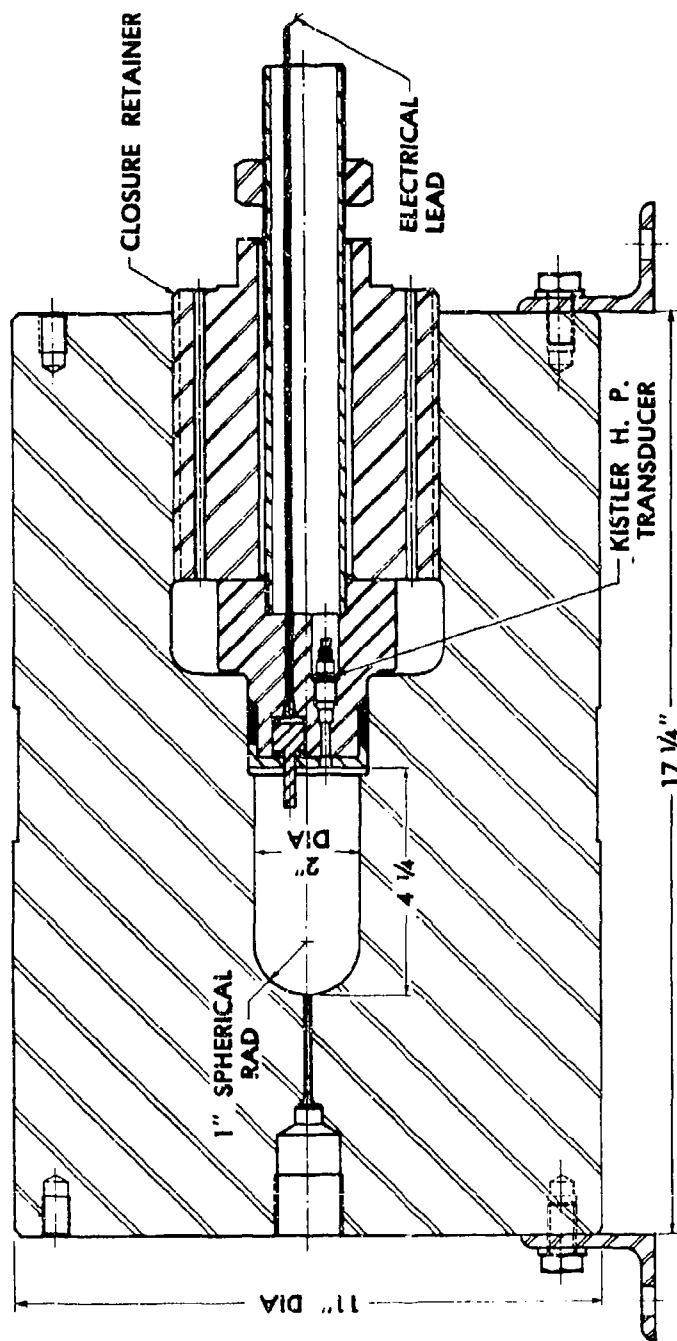


Figure 1. High Pressure Closed Chamber Used for Propellant Testing



Figure 2. Typical Charge Configuration With Coil Assembly

were closed by tying the cellophane bag around the match leads with dacron thread. For calculation purposes, the mass of each component in the charge was recorded (dacron, match, CBI, cellophane, propellant). Loading of the closed bomb fixture was accomplished by attaching the charge leads to the firing electrode, placing the appropriate coils around the charge, and inserting the entire assembly as a unit. The exceptions to this were the M-10 and the NOSOL 363 both at  $s/v$  of  $5 \text{ cm}^{-1}$  and loading densities of  $0.4 \text{ g/cc}$  and  $0.3 \text{ g/cc}$  respectively. These samples were, by necessity, prepared by enclosing the coils in the cellophane with the charge. Each matrix element was assigned a number and a random number generator was used to determine shot order. Sample weights ranged from  $17.5 \text{ g}$  to  $84.0 \text{ g}$  to give loading densities from  $0.1 \text{ g/cc}$  to  $0.4 \text{ g/cc}$ .

### III. RESULTS & DISCUSSION

The two propellants used in the experiment: a single base, fast burning M-10 (web= $0.058 \text{ cm}$ ) and the two samples of a slower burning, double base NOSOL 363 (web= $0.271$  &  $0.081 \text{ cm}$ ), showed the same trends for the various comparisons that were done. The constant heat loss option reductions show little change in the extracted burning rates from varying either  $s/v$  or loading density. The reductions done using the proportional heat loss option show a continual increase in slope at constant loading density as  $s/v$  increases. Differences start to show up between the constant and proportional options as  $s/v$  increases past one. Experimental results from use of the brass coil turned out as expected. The reductions of the shots using brass at  $s/v$  of three were very similar to those using steel coils at  $s/v$  of five.

We expected the maximum pressure to decrease, as  $s/v$  increased at the same loading density, due to the increased surface area extracting more heat from the chamber gases during the pressure rise. The initial results indicated that, indeed, the experiment did work in the expected manner. As can be seen in Table 1, as  $s/v$  increased at any constant loading density, the maximum pressure obtained decreased.

The CBRED2 data reduction program gives results in graphical form of burn rate vs. pressure. Graphs can be produced on log-log plots to give the burning rate exponent but as we were doing a comparative study, the decision was made to use linear scales here as the log-log scales can mask discrete variations in the burn rate. All of the data was reduced using both of the heat loss options available, constant and proportional. A few shots were also reduced with the assumption that there was no heat loss. The multiple heat loss reductions were decided upon after seeing the initial data reduction results, mentioned in the previous paragraph. Three repetitions of each matrix option were fired and average plots were constructed from plot overlays within each option. The data was then compared by overplotting the various data sets. Each one of the variables: heat loss, loading density, and  $s/v$  was studied while keeping the other two constant.

The derived burn rates of the data, reduced using the constant heat loss option, show good agreement as the  $s/v$  changes at a constant loading density. This can be seen by examining Fig. 3. The agreement is especially good at  $0.3 \text{ g/cc}$ , which gives a maximum pressure similar to what a large

TABLE 1. THE AVERAGE MAXIMUM PRESSURE (MPa) AT EACH MATRIX OPTION  
FROM THE M-10 SHOT WITH THE STEEL COILS

<u>s/v</u>	<u>LOADING DENSITY (g/cc)</u>			
(cm <sup>-1</sup> )	0.1	0.2	0.3	0.4
1	120.9	266.5	443.9	662.1
2	116.0	257.1	442.8	654.7
3	111.9	253.2	438.8	652.2
5	108.0	247.5	424.9	653.7

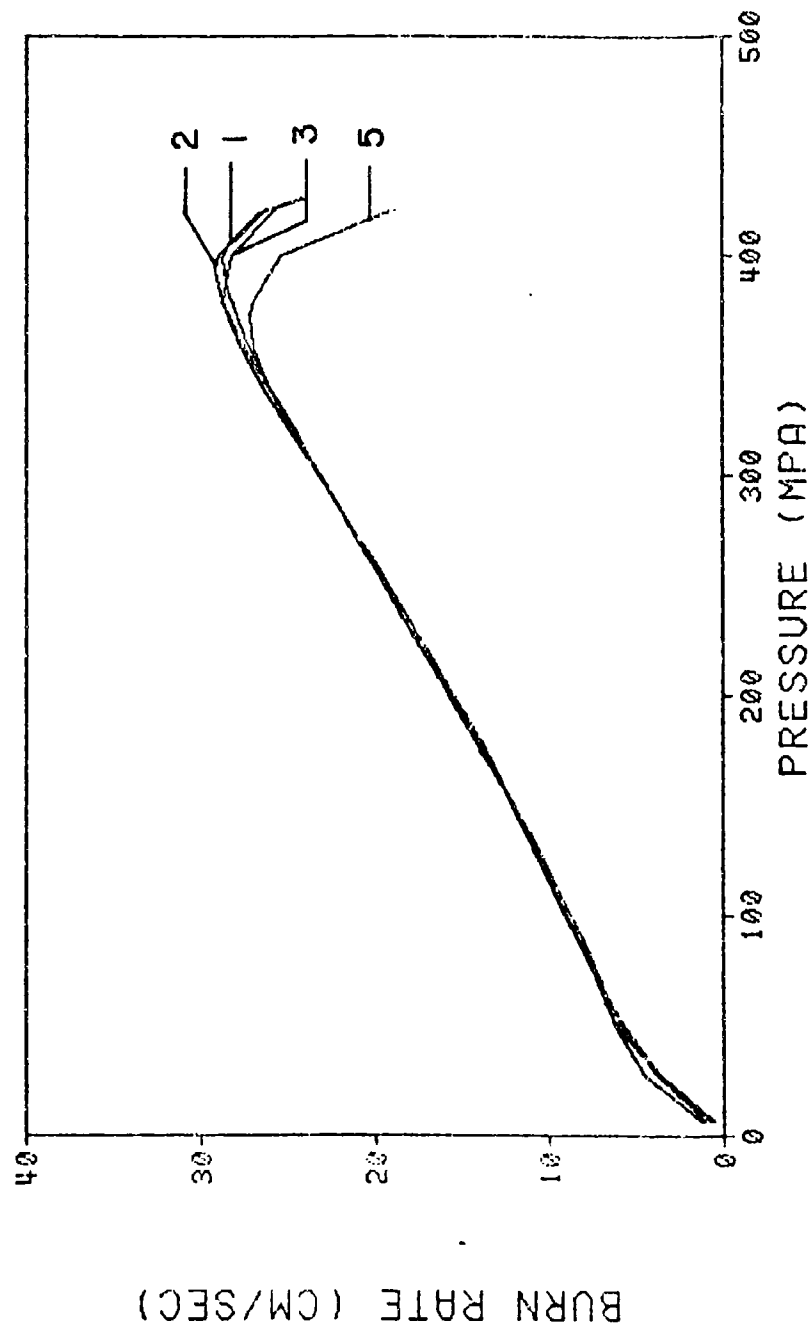


Figure 3. Overplots Showing Constant Loading Density at 0.3 g/cc with  $s/v$  of 1, 2, 3, & 5  $\text{cm}^{-1}$ . All Data Reduced Using the Constant Heat Loss Option.

caliber gun typically experiences. When the data is compared at constant s/v over all loading densities, the burn rates again compare favorably. As Fig. 4 shows, the slopes at loading densities of 0.2, 0.3, and 0.4 g/cc are virtually identical. The slopes at 0.1 g/cc vary from the others, but the correlation at this loading density is seldom good. Any amount of ignition delay, but especially long ones, can have large effects at such a low loading density. It may be possible to input tabular, rather than average, thermochemicals and get better agreement.

The derived burn rates of the data reduced using the proportional heat loss option do not agree as well as those from the constant heat loss option. These burn rates increase 10%-12% as s/v changes from one to five at any one loading density (see Fig. 5). When the data obtained at the various loading densities is compared at constant s/v ratios, the slope decreases about 8% at s/v of 5 cm<sup>-1</sup> as the loading density goes from 0.1 to 0.4 g/cc (see Fig. 6). At s/v of 1 cm<sup>-1</sup>, the slopes remain almost constant as the loading density changes.

The overall differences in the results between the constant and proportional heat loss options are interesting. Close examination of the proportional results shows that there is a small but distinct slope change, or dip, in the regime of the maximum mass generation rate. As the s/v ratio increases, this variation in slope also increases. This is to be expected when one takes into consideration how the heat loss coefficient affects the mass generation rate in the data reduction program.

The equation below represents the rate of conversion of solid to gas (mass burning rate) in CBRED2.

$$dwp/dt = (A + B) / R_s T_{op} - P[1/\rho] - \eta]$$

where:

$R_s$  = gas constant for the system

$T_{op}$  = isochoric adiabatic propellant flame temperature

$P$  = pressure

$\eta$  = propellant covolume

$\rho$  = propellant density

$A = V_s \frac{dP}{dt}$  (System Volume Term)

$B = H_L (\gamma - 1)$  (Heat Loss)

As can be seen, the computed mass burning rate increases if the heat loss term (B) increases. In the constant heat loss option, the value of B remains the same throughout the reduction. For the proportional option, that same heat loss term increases when the instantaneous mass flow increases, which implies that the two terms feed each other. If the heat loss term can be drastically increased, as in our experiment, by purposely

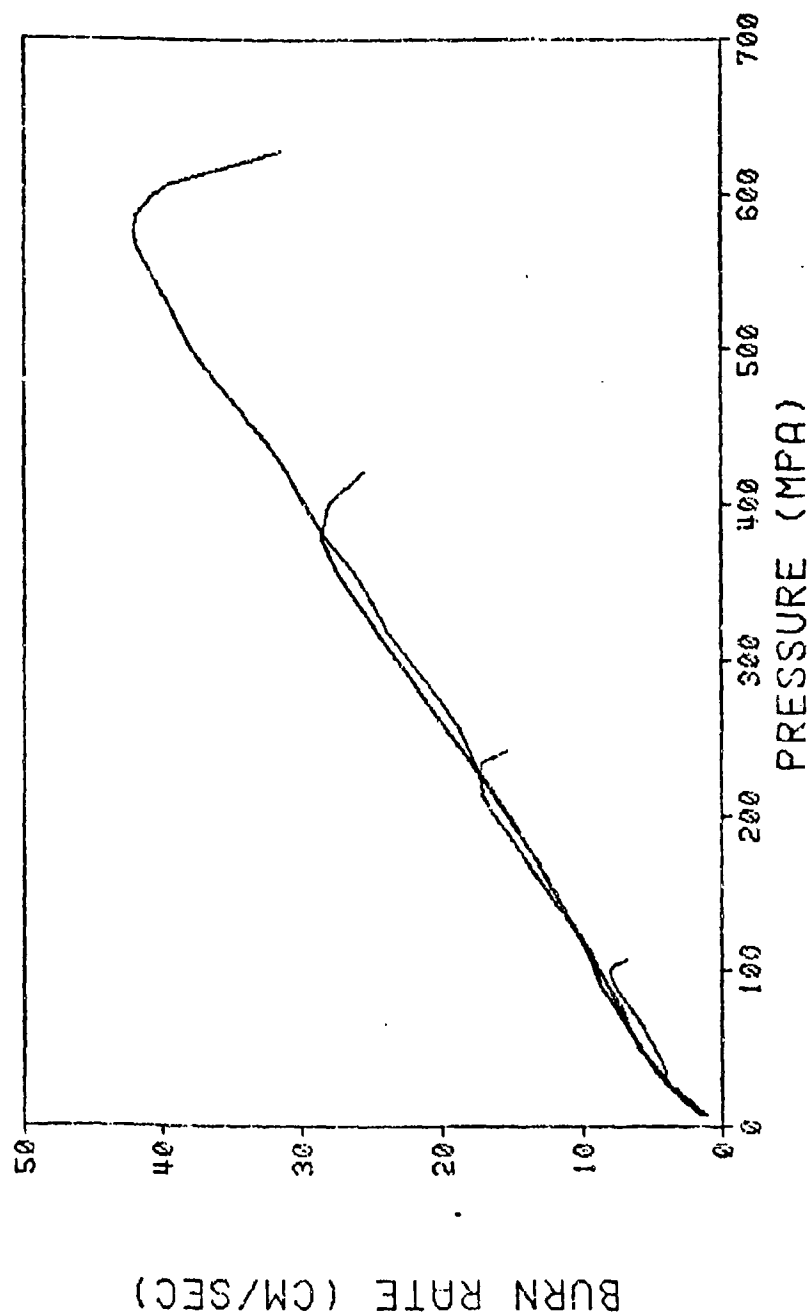


Figure 4. Overplots Showing Constant  $s/v$  of  $3 \text{ cm}^{-1}$  with Loading Densities at 0.1, 0.2, 0.3, & 0.4 g/cc. All Data Reduced Using the Constant Heat Loss Option.



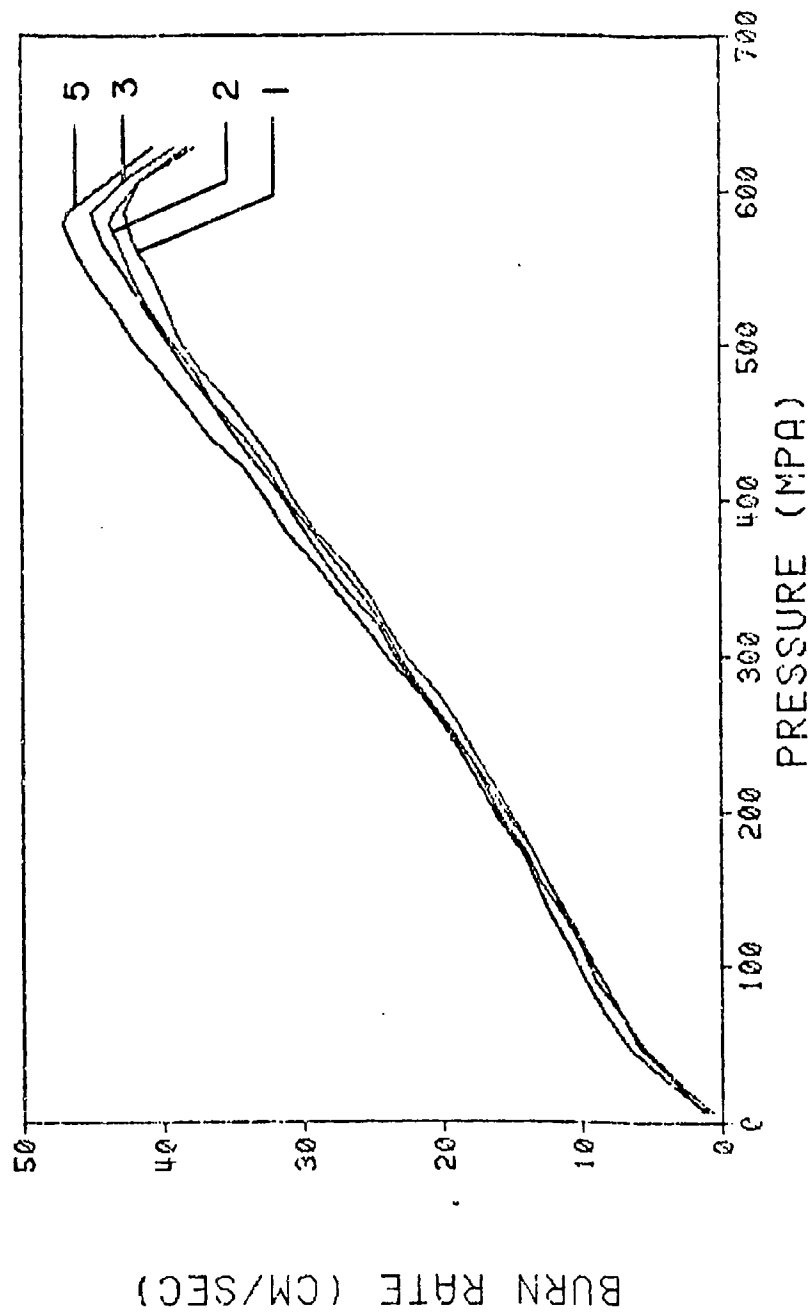


Figure 5. Overplots Showing Constant Loading Density at 0.4 g/cc with  $s/v$  of 1, 2, 3, & 5  $\text{cm}^{-1}$ . All Data Reduced Using the Proportional Heat Loss Option.

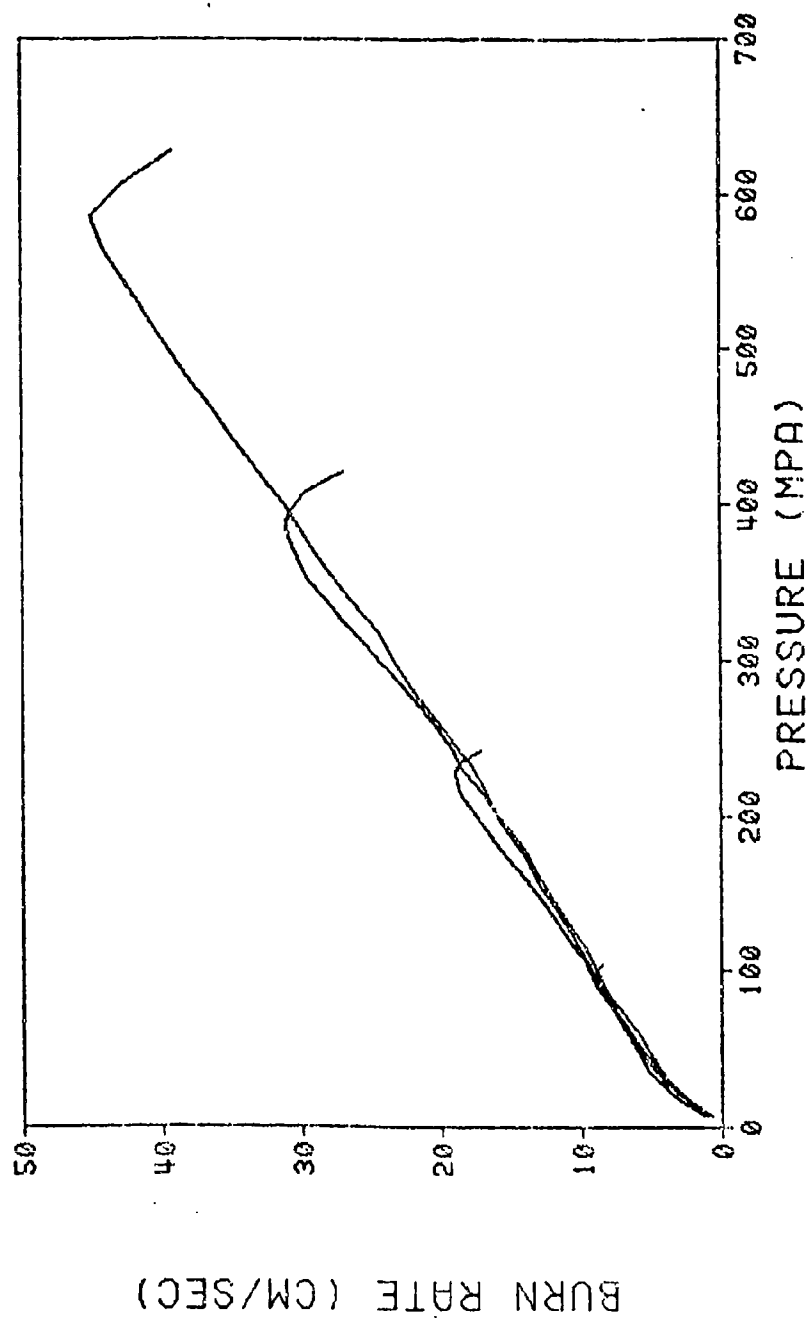


Figure 6. Overplots Showing Constant  $s/v$  of  $3 \text{ cm}^{-1}$  with Loading Densities at 0.1, 0.2, 0.3, & 0.4 g/cc. All Data Reduced Using the Proportional Heat Loss Option.

introducing coils to increase the surface area available for heat transfer, then the computed burning rate will be artificially elevated at high mass generation rates.

Comparisons of the constant and proportional heat loss options show little difference at  $s/v$  of one. In fact, one of the matrix options was reduced assuming no heat loss and the resultant burning rate curve is indistinguishable from either the constant or proportional option (see Fig. 7). As  $s/v$  increases, however, the proportional option continually shows an increase in burning rate; relative to the constant option (see Fig. 8). This is as much as 17% at  $s/v$  of five.

The above results suggest that, with CBRED2 and possibly other data reduction programs, closed bomb burning rate data, obtained with vessels with "low"  $s/v$  values, is not very sensitive to heat loss treatment. However, the rules appear to get modified as the  $s/v$  increases past  $2 \text{ cm}^{-1}$ . This is fortunate because typical closed bombs have a  $s/v$  of less than two. All the closed bombs used in the round robin exercise had a  $s/v$  of close to  $1 \text{ cm}^{-1}$ . Closed bombs in use at the Ballistic Research Laboratory (with the exception of the 0.50 cal. fixture mentioned in the introduction) all have a  $s/v$  between 0.8 and  $1.7 \text{ cm}^{-1}$ . For example, our main 200 cc bomb is 10.5 cm long and 5.1 cm in diameter to give a  $s/v$  of  $0.92 \text{ cm}^{-1}$ . The primary 700 cc vessel has an inside cavity 34 cm long with a diameter of 5.1 cm to give a  $s/v$  of  $0.85 \text{ cm}^{-1}$ . According to these results and the bombs we presently have in operation, using either one of the heat loss options should give us valid burning rate data.

Significantly, it was this program, CBRED2, that was used by the BRL for its contributions to the JANNAF Round Robin. Those results were in good agreement with the other closed bomb results as well as the strand burner data that was presented. The CBRED2 burning rate data, therefore, has been "calibrated" against other data reduction techniques as well as against directly measured burning rate values. Any effects we may have observed here at high  $s/v$  values for the proportional option are negligible under normal closed bomb conditions.

Up to this point, all of the results have been taken from data obtained by shooting M-10, with and without steel coils. The burning rates computed with the constant heat loss option all show good slope agreement and little sensitivity to large changes in  $s/v$  value. The proportional option, while being much more rigorous in its heat loss treatment, appears to have some sensitivity to fairly large  $s/v$  changes. The two reductions that were done assuming no heat loss were not sufficient to get any real trends, but at  $0.2 \text{ g/cc}$  and  $1 \text{ cm}^{-1}$  the results were almost identical to the other two options.

After observing the results from the M-10 firings, which used a single base propellant with a small web to give a fast burning granulation, the decision was made to increase the matrix using a slower propellant. Some unusual effects have been observed on the burning rates of very slow burning grains and we were interested in finding out how the increase in  $s/v$  would influence results from a slower burning charge. The propellant selected was

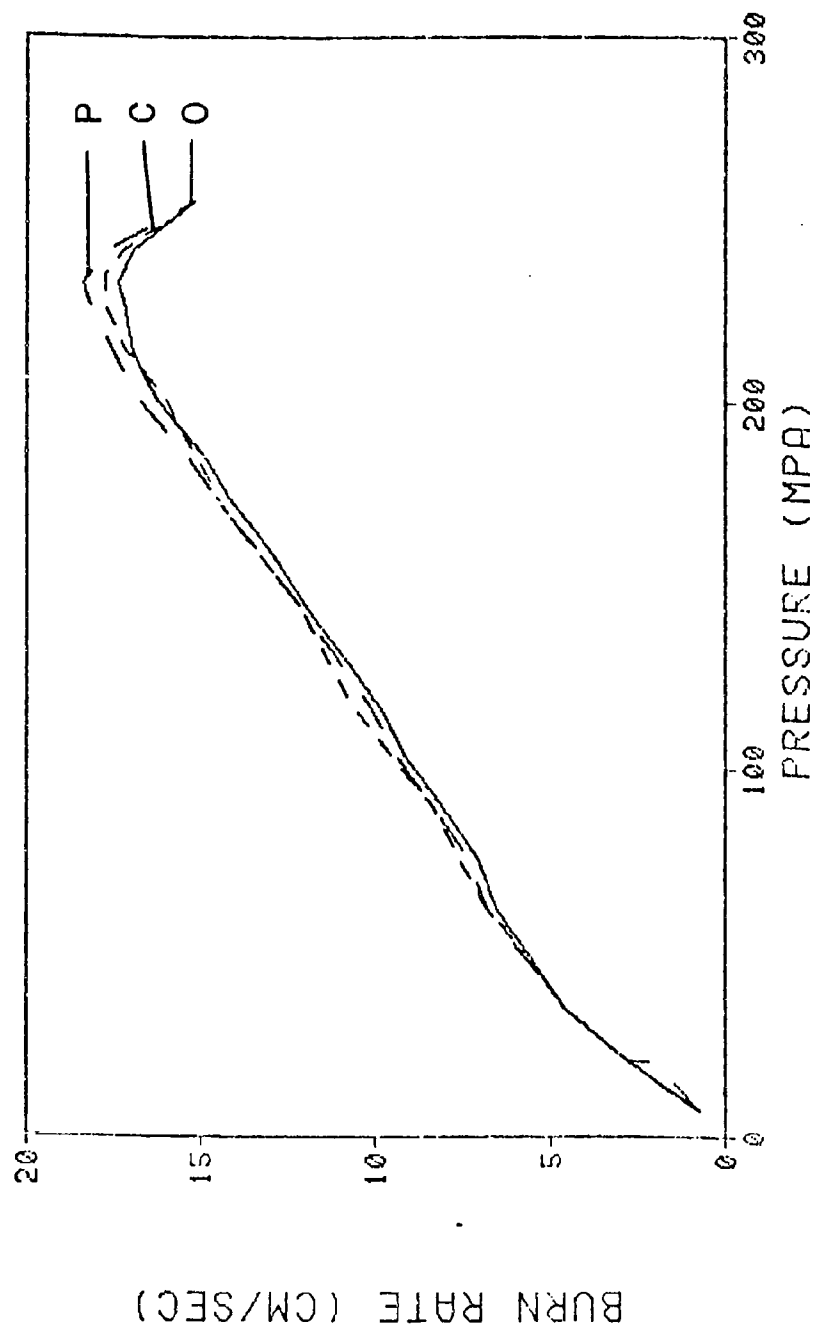


Figure 7. Overplots Showing Constant Loading Density at 0.2 g/cc and Constant  $s/v$  of  $1 \text{ cm}^{-1}$ . Data Reduced Using the Proportional (P), Constant (C), and Zero (O) Heat Loss Options.

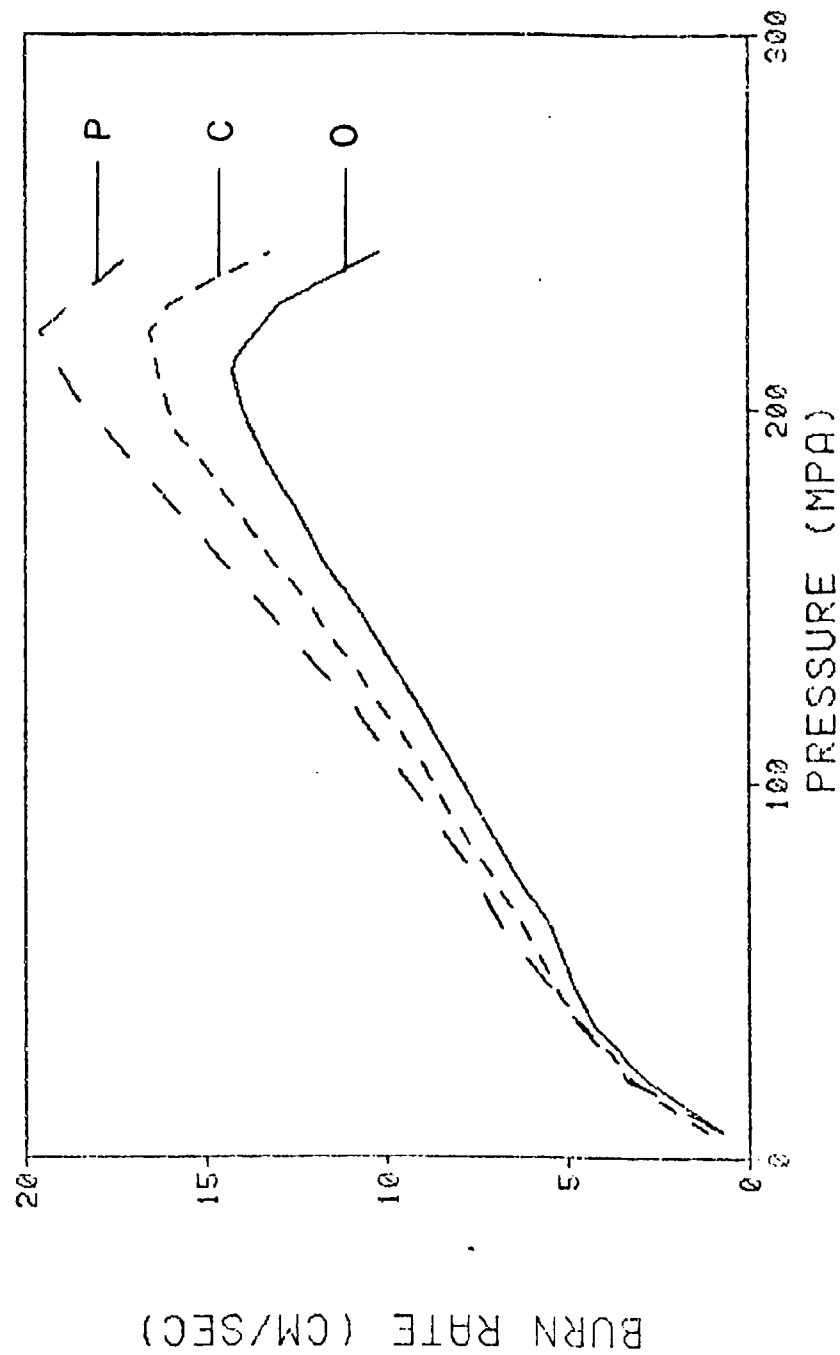


Figure 8. Overplots Showing Constant Loading Density at 0.2 g/cc and Constant  $s/v = 5 \text{ cm}^{-1}$ . Data Reduced Using the Proportional (P), Constant (C), and Zero (O) Heat Loss Options.

some single perforated NOSOL 363 extruded in two different web sizes (0.081 cm & 0.271 cm) from the same lot. We decided to incorporate both of them into the matrix at 0.3 g/cc and s/v ratios of 1 & 5 cm<sup>-1</sup>. The reduced burning rates (but not the burn times) of the two different sized NOSOL 363 samples were identical. The proportional options showed a very slight increase in slope over the constant options at s/v of 1 cm<sup>-1</sup>, and a 12% increase at s/v of 5 cm<sup>-1</sup>. This compares well with the results from the M-10 comparisons and may indicate that the heat loss options are consistent, between fast and slow propellants, in their results.

A note of caution is in order concerning our interpretation of the NOSOL 363 data. The M-10 went from 10%-90% P<sub>max</sub> in about 1.5 milliseconds. The NOSOL 363 with the large web covered the same event in about 9.5 milliseconds. We are examining the possibility that the infinite heat sink assumption was not valid over the increased time spans.

Our local discrepancy between the computed burning rate data obtained in the 200 cc bomb and the fixture made from the breech section of a 0.50 caliber gun was still disturbing. Was it possible that increased thermal conductivity from the brass cartridge case could be responsible for the increase in computed burn rates? The decision was made to replace the steel coils with a brass coil for shots with the M-10 at 0.3 g/cc and s/v of 1 and 3 cm<sup>-1</sup>. The results showed almost no difference from the burning rate curves reduced from the steel coil firings. The constant option results that came from using the brass coil were identical to those from the steel coils. The proportional results from the brass coils at a s/v of three were very close to the results from the steel coils at a s/v of five. This was as expected due to the higher thermal diffusivity of the brass. At this time, the initial discrepancy between the results is still unexplained.

For all this discussion on derived burn rates, the primary purpose of the data is to predict gun system performance. To that end, we took various closed bomb burning rate data from this study and keyed it into an interior ballistic code for input into a 105-mm system. All of the burning rate data came from a loading density of 0.3 g/cc. The s/v ratios were at one, three, and five cm<sup>-1</sup>. The constant and proportional heat loss options were used so we had six sets of burning rate data that were varied while the rest of the parameters in the 105-mm system remained constant. Four of the data sets had less than a 1% change in peak pressure and muzzle velocity. These were the three constant heat loss reductions and the one proportional option at s/v of 1 cm<sup>-1</sup>. Input of data from the proportional option at s/v of 3 cm<sup>-1</sup> showed an increase of 8% in peak pressure and a 3% increase in muzzle velocity over the data from s/v of 1 cm<sup>-1</sup>. The amount of increase was greater, 17% and 4% respectively, at s/v of 5 cm<sup>-1</sup>.

These figures serve to point out that, for closed bomb burning rate data used for interior ballistic predictions, heat loss problems may be minimized by the use of a vessel with a s/v near 1 cm<sup>-1</sup> and treating the heat loss factor in a simplistic manner. Conversely, gun performance predictions may be seriously affected by the use of derived burning rate data obtained with a vessel having a large s/v.

#### IV. CONCLUSIONS & RECOMMENDATIONS

While the reduction of closed bomb data is not a simple task, the heat loss aspect of the reduction does not seem to be a very sensitive area. This is provided that the vessel in use for the closed bomb operation has a low surface area to volume ratio and the propellant fired has fairly rapid burning rate. It may be possible to extend this observation to much slower granulations but further experimentation is necessary.

#### ACKNOWLEDGEMENTS

Special acknowledgements go to; H. Goodman, for assistance rendered with the interior ballistic calculations, and Dr. E. Freedman, for allowing us to use the data from his experiment as a base for this study.



## REFERENCES

1. C. Price and A. Juhasz, "A Versatile User-Oriented Closed Bomb Data Reduction Program (CBRED)," Ballistic Research Laboratories Report, BRL Report No. 2018, September, 1977.
2. F.W. Robbins and A.W. Horst, "Numerical Simulation of Closed Bomb Performance Based on BLAKE Code Thermodynamic Data," Indian Head Memorandum Report, IHMR 76-259, November, 1976.
3. H. Krier, "Extracting Burning Rates For Multiperforated Propellant From Closed Bomb Testing," Aeronautical and Astronautical Engineering Department, University of Illinois at Urbana-Champaign, Technical Report AAE 78-2, UILU-ENG 78-0502, July, 1978.
4. S. Mitchell and A. Horst, "Comparitive Burning Rate Study," CPIA Publication 281, Bulletin of the 13th JANNAF Combustion Meeting, Chemical Propulsion Information Agency, Johns Hopkins University/Applied Physics Laboratory, September, 1976.
5. A.A. Juhasz, ed., "Round Robin Results of the Closed Bomb and Strand Burner," Applied Physics Laboratory, CPIA Publication 361, July, 1982.

## APPENDIX

After the initial presentation of this paper at the 21st JANNAF Combustion Meeting, some ideas and observations were brought up by some members of the propellant community.

### A. Data Presentation

An alternate method of presenting the data was proposed, plotting  $s/v$  ratios versus burning rates at various pressures. It was argued that plotting the data in such a way would more readily reveal the surface area effects on the derived burning rates. Two plots of this method of data presentation are shown in Figures A-1 and A-2. As can be seen in Figure A-1, which plots  $s/v$  vs. burn rate at 0.3 g/cc for the constant heat loss option, the lines maintain a constant slope of zero at all pressures. The constant zero slope indicates no  $s/v$  effects on the derived burning rates. In Figure A-2, however, in which data are plotted from the proportional heat loss options, an increase in slope is noted, indicating a dependence of derived burning rate on  $s/v$  ratio. The proposed method of presentation, as suggested, highlights the observed differences for the burning rate vs.  $s/v$  effects.

### B. Tabular Thermochemical Input and Proportional Heat Loss Option

The suggestion was also made that the discrepancies between the derived burning rates, which increased as the  $s/v$  increased, could be reduced through the use of the tabular thermochemical input option in CBRED when using the proportional heat loss option.

Figure A-3 compares the derived burning rates from the reductions that had a loading density of 0.3 g/cc and  $s/v=1 \text{ cm}^{-1}$ . The figure indicates that, while there is no apparent difference between the proportional and constant heat loss options using average thermochems, the use of tabular thermochemistry does show a slight difference at a  $s/v$  of  $1 \text{ cm}^{-1}$ . The comparison of data from the experiments that had a  $s/v$  of  $5 \text{ cm}^{-1}$  can be observed in Figure A-4. This plot indicates that the use of tabular thermochemical input decreases the discrepancy between the derived burning rates computed via average thermochemistry with either the constant or proportional heat loss option. Finally, Figure A-5 compares the derived burning rate results from data taken with a  $s/v$  of  $1 \text{ cm}^{-1}$  and  $5 \text{ cm}^{-1}$ , and reduced using the proportional heat loss option and tabular thermochemical input. The derived burning rate data from  $s/v$  of  $5 \text{ cm}^{-1}$  still falls above that from  $s/v$  of  $1 \text{ cm}^{-1}$ , although the spread is about half as great as that from similar reductions using average thermochemistry.

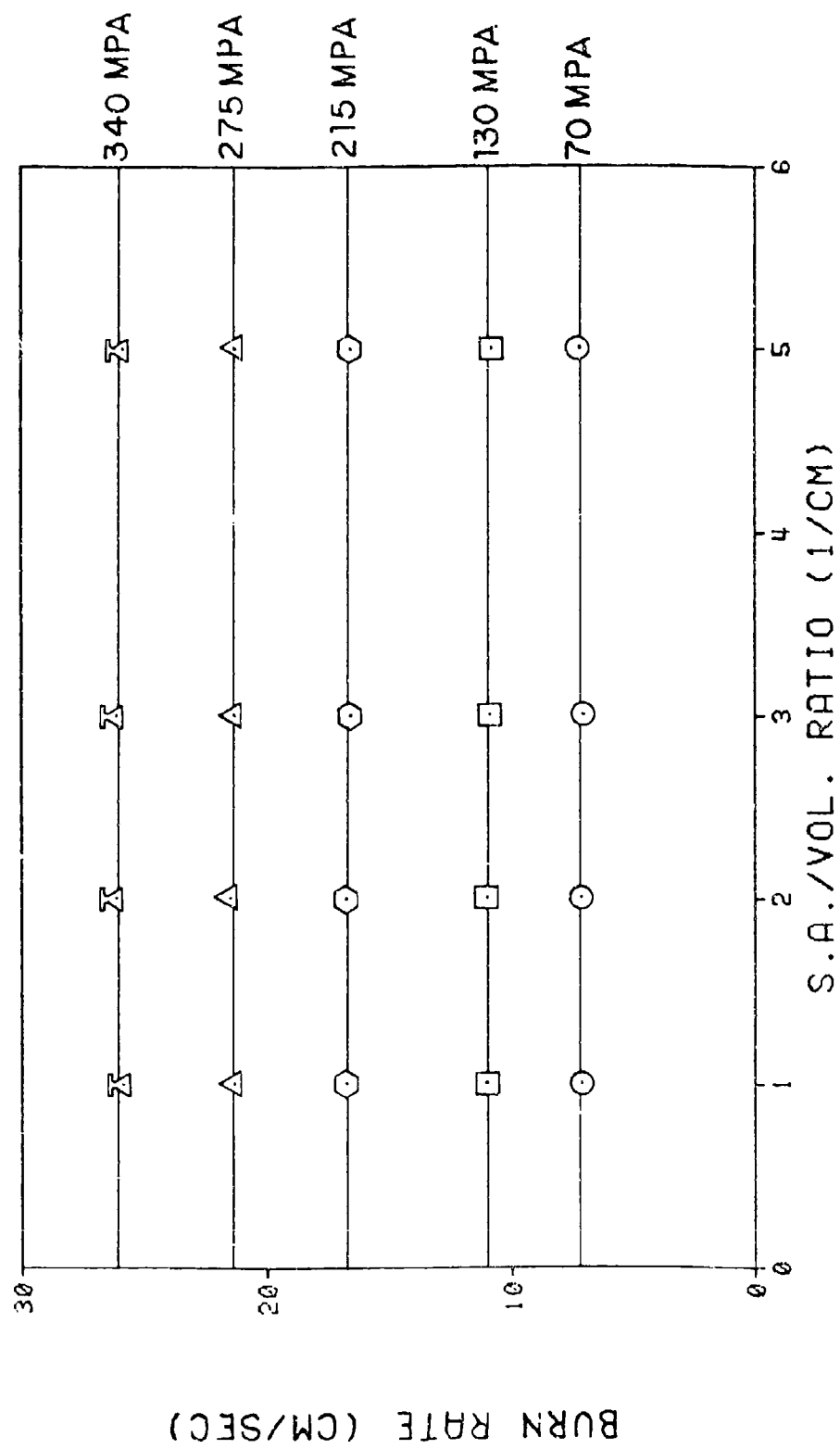


Figure A-1. Constant heat loss option. Superimposed plots of s/v ratio vs Burn Rate.

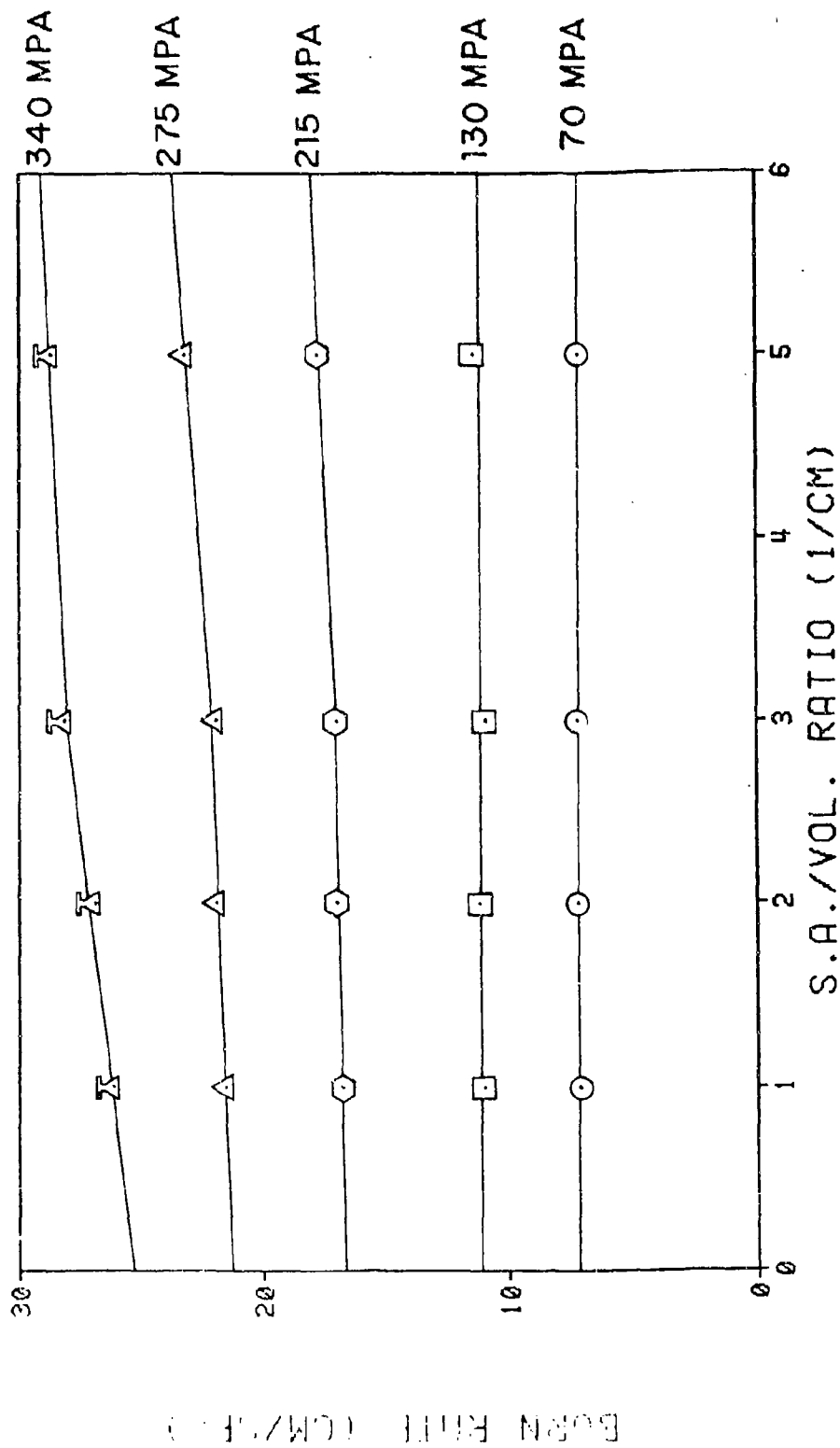


Figure A-2. Proportional heat loss option. Superimposed plots of s/v ratio vs Burn Rate.

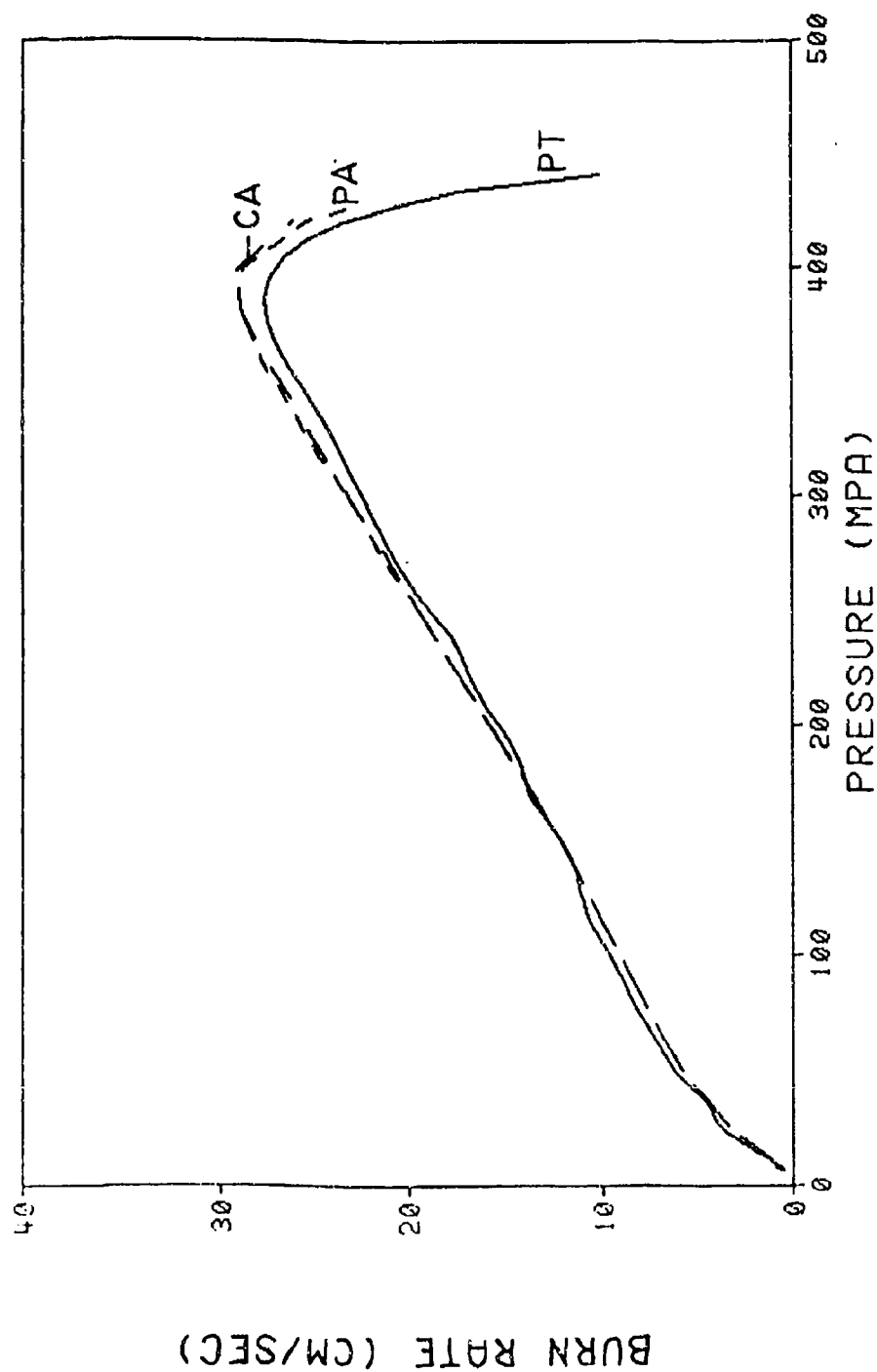


Figure A-3. All heat loss options. Superimposed burning rate plots at 0.3 g/cc and  $s/v = 1 \text{ cm}^{-1}$ . Data reduced using; proportional heat loss option & tabular thermochemicals (PT), proportional heat loss option & average thermochemicals (PA), constant heat loss option & average thermochemicals (CA).

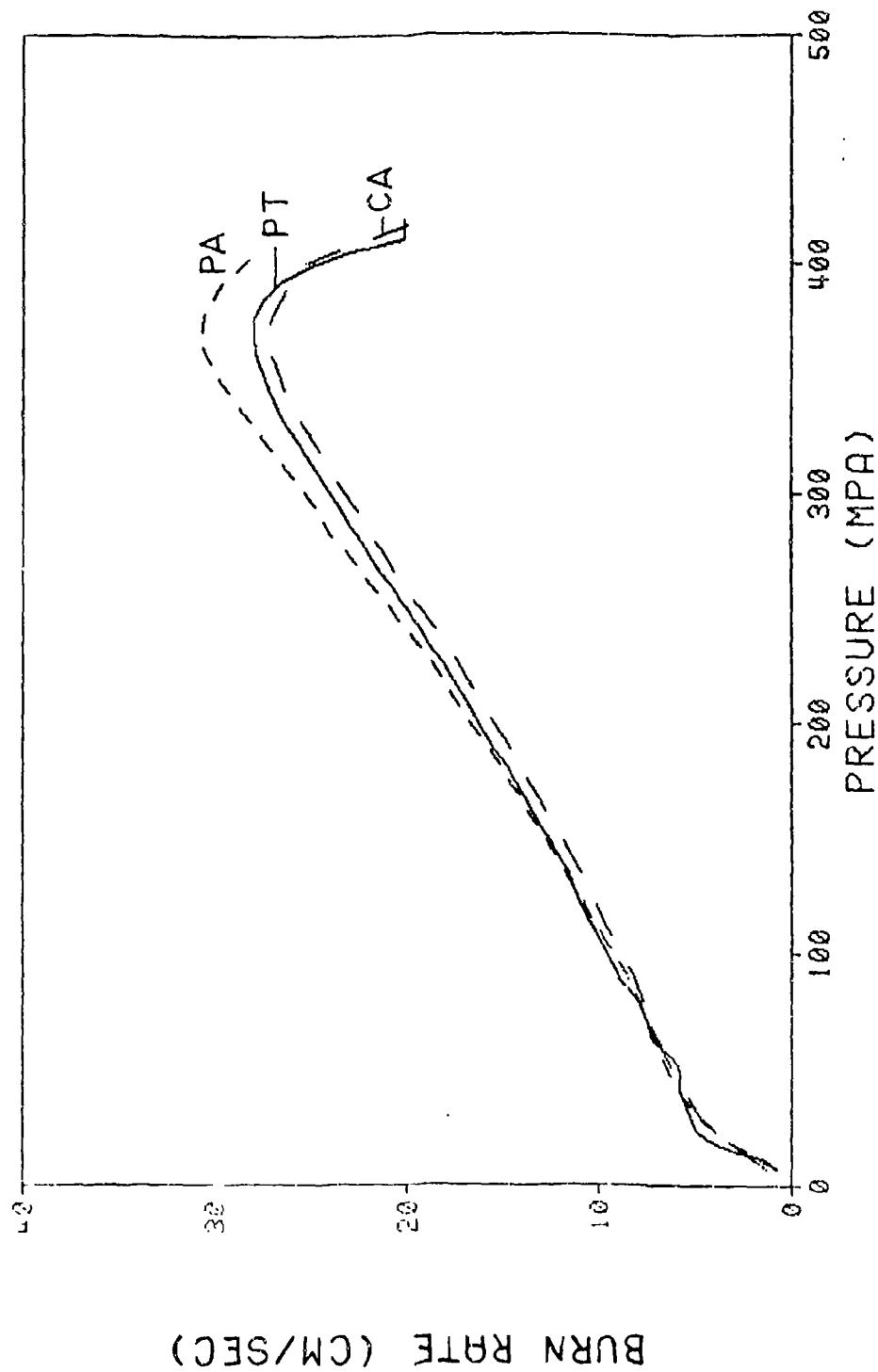


Figure A-4. All heat loss options. Superimposed burning rate plots at 0.3 g/cc and  $s/v = 5 \text{ cm}^{-1}$ . Data reduced using; proportional heat loss option & tabular thermochemicals (PT), proportional heat loss option & average thermochemicals (PA), constant heat loss option & average thermochemicals (CA).

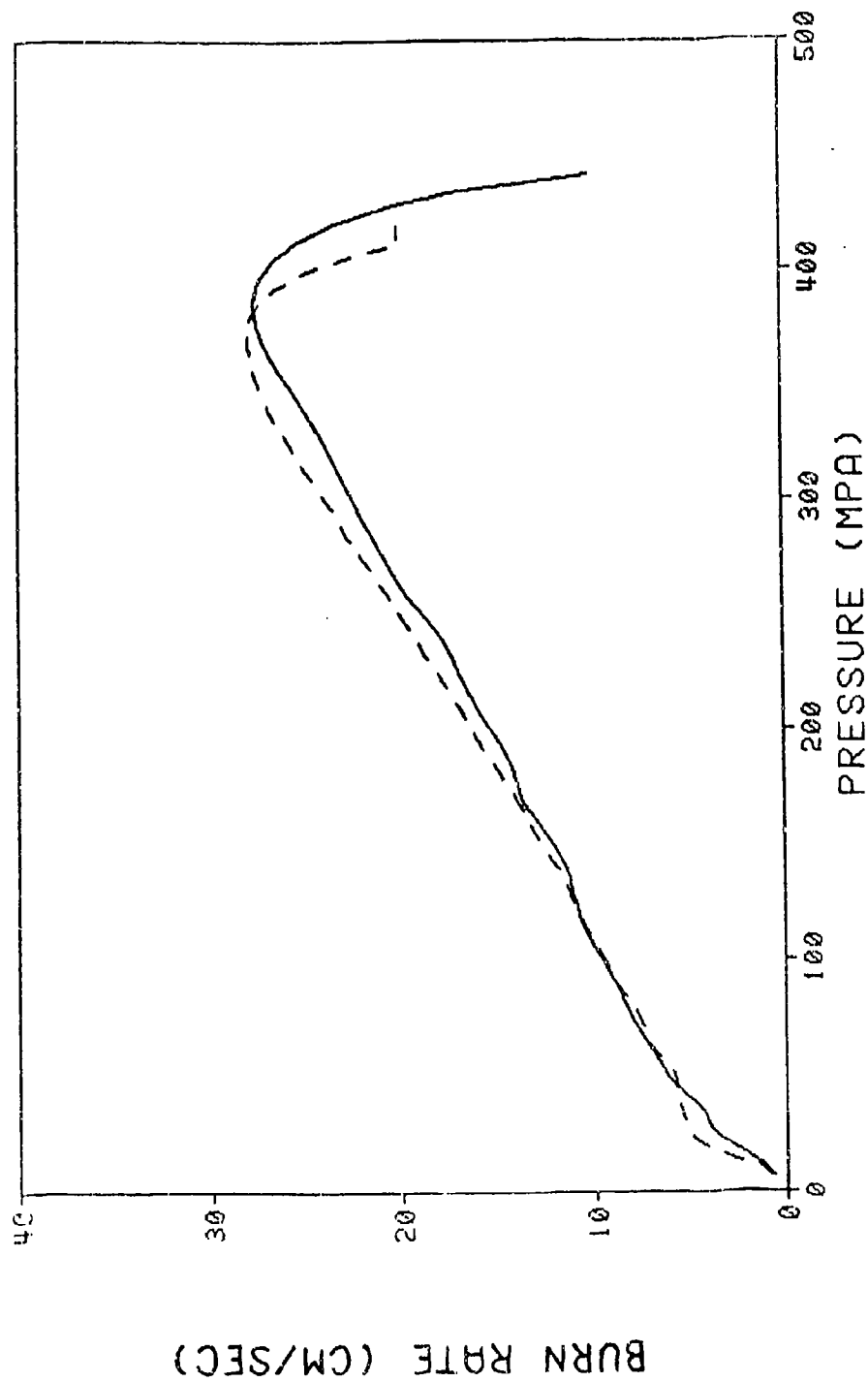


Figure A-5. Proportional heat loss option & tabular thermochems. Superimposed burning rate plots at 0.3 g/cc with  $s/v = 1 \text{ cm}^{-1}$  (solid line) and 0.3 g/cc with  $s/v = 5 \text{ cm}^{-1}$  (dotted line).

# DISTRIBUTION LIST

<u>No. Of Copies</u>	<u>Organization</u>	<u>No. Of Copies</u>	<u>Organization</u>
12	Commander Defense Technical Info Center ATTN: DTIC-DDA Cameron Station Alexandria, VA 22304-6145	1	Commander US Army Materiel Command ATTN: AMCDRA-ST 5001 Eisenhower Avenue Alexandria, VA 22333-0001
1	Commander USA Concepts Analysis Agency ATTN: D. Hardison 8120 Woodmont Avenue Bethesda, MD 20014	5	Project Manager Cannon Artillery Weapons System, ARDC, AMCCOM ATTN: AMCPM-CW, F. Menke AMCPM-CWW AMCPM-CWS M. Fisette AMCPM-CWA R. DeKleine H. Hassmann Dover, NJ 07801
1	HQDA/DAMA-ZA Washington, DC 20310		
1	HQDA, DAMA-CSM, E. Lippi Washington, DC 20310		
1	HQDA/DAMA-ART-M Washington, DC 20310	2	Project Manager Munitions Production Base Modernization and Expansion ATTN: AMCPM-PBM, A. Siklosi AMCPM-PBM-E, L. Laibson Dover, NJ 07801
1	HQDA/SARDA Washington, DC 20310		
1	Commander US Army War College ATTN: Library-FF229 Carlisle Barracks, PA 17013	3	Project Manager Tank Main Armament System ATTN: AMCPM-TMA, K. Russell AMCPM-TMA-105 AMCPM-TMA-120 Dover, NJ 07801
1	Director US Army BMD Advanced Technology Center P. O. Box 1500 Huntsville, AL 35807	1	Commander US Army Watervliet Arsenal ATTN: SARVV-RD, R. Thierry Watervliet, NY 12189
1	Chairman DOD Explosives Safety Board Room 856-C Hoffman Bldg. 1 2461 Eisenhower Avenue Alexandria, VA 22331		



# DISTRIBUTION LIST

<u>No. Of Copies</u>	<u>Organization</u>	<u>No. Of Copies</u>	<u>Organization</u>
22	Commander US Army ARDC, AMCCOM ATTN: SMCAR-TSS SMCAR-TDC SMCAR-LC LTC N. Barron SMCAR-LCA A. Beardell D. Downs S. Einstein S. Westley S. Bernstein P. Kemmey A. Bracuti J. Rutkowski SMCAR-LCB-1 D. Spring SMCAR-LCE, R. Walker SMCAR-LCM-E S. Kaplowitz SMCAR-LCS SMCAR-LCU-CT E. Barrieres R. Davitt SMCAR-LCU-CV C. Mandala SMCAR-LCW-A M. Salisbury SMCAR-SCA L. Stiefel B. Brodman Dover, NJ 07801	1	Director Benet Weapons Laboratory Armament R&D Center US Army AMCCOM ATTN: SMCAR-LCB-TL Watervliet, NY 12189
		1	Commander US Army Aviation Research and Development Command ATTN: AMSAV-E 4300 Goodfellow Blvd. St. Louis, MO 63120
		1	Commander US Army TSARCOM 4300 Goodfellow Blvd. St. Louis, MO 63120
		1	Director US Army Air Mobility Research And Development Laboratory Ames Research Center Moffett Field, CA 94035
		1	Commander US Army Communications Electronics Command ATTN: AMSEL-ED Fort Monmouth, NJ 07703
		1	Commander ERADCOM Technical Library ATTN: DELSD-L Fort Monmouth, NJ 07703-5301
4	Commander US Army Armament Munitions and Chemical Command ATTN: SMCAR-ESP-L L. Ambrosini AMSMC-IRC, G. Cowan AMSMC-LEM W. Fortune R. Zastrow Rock Island, IL 61299	1	Commander US Army Harry Diamond Lab. ATTN: DELHD-TA-L 2800 Powder Mill Road Adelphi, MD 20783
		1	Commander U.S. Army Missile Command Research, Development & Engineering Center ATTN: AMSMI-RD Redstone Arsenal, AL 35898

# DISTRIBUTION LIST

<u>No. Of Copies</u>	<u>Organization</u>	<u>No. Of Copies</u>	<u>Organization</u>
1	Commander U.S. Army Missile & Space Intelligence Center ATTN: ALAMS-YDL Redstone Arsenal, AL 35898-5500	1	Project Manager M-60 Tank Development ATTN: AMCPM-M60TD Warren, MI 48090
1	Commandant US Army Aviation School ATTN: Aviation Agency Fort Rucker, AL 36360	1	Director US Army TRADOC Systems Analysis Activity ATTN: ATAA-SL White Sands Missile Range, NM 88002
1	Commander US Army Tank Automotive Command ATTN: AMSTA-TSL Warren, MI 48090	1	Commander US Army Training & Doctrine Command ATTN: ATCD-MA/ MAJ Williams Fort Monroe, VA 23651
1	Commander US Army Tank Automotive Command ATTN: AMSTA-CG Warren, MI 48090	2	Commander US Army Materials and Mechanics Research Center ATTN: AMXMR-ATL Tech Library Watertown, MA 02172
1	Project Manager Improved TOW Vehicle ATTN: AMCPM-ITV US Army Tank Automotive Command Warren, MI 48090	1	Commander US Army Research Office ATTN: Tech Library P. O. Box 12211 Research Triangle Park, NC 27709-2211
2	Program Manager M1 Abrams Tank System ATTN: AMCPM-GMC-SA, T. Dean Warren, MI 48090	1	Commander US Army Belvoir Research & Development Center ATTN: STRBE-WC Fort Belvoir, VA 22060-5606
1	Project Manager Fighting Vehicle Systems ATTN: AMCPM-FVS Warren, MI 48090	1	Commander US Army Logistics Mgmt Ctr Defense Logistics Studies Fort Lee, VA 23801
1	President US Army Armor & Engineer Board ATTN: ATZK-AD-S Fort Knox, KY 40121		

# DISTRIBUTION LIST

<u>No. Of Copies</u>	<u>Organization</u>	<u>No. Of Copies</u>	<u>Organization</u>
1	Commandant US Army Infantry School ATTN: ATSH-CD-CSO-OR Fort Benning, GA 31905	1	General Applied Sciences Lab ATTN: J. Erdos Merrick & Stewart Avenues Westbury, NY 11590
1	President US Army Artillery Board Ft. Sill, OK 73503	1	Office of Naval Research ATTN: Code 473, R. S. Miller 800 N. Quincy Street Arlington, VA 22217
1	Commandant US Army Command and General Staff College Fort Leavenworth, KS 66027	2	Commander Naval Sea Systems Command ATTN: SEA 62R SEA 64 WashLugton, DC 20362-5101
1	Commandant US Army Special Warfare School ATTN: Rev & Tng Lit Div Fort Bragg, NC 28307	1	Commander Naval Air Systems Command ATTN: AIR-954-Tech Lib Washington, DC 20360
3	Commander Radford Army Ammo Plant ATTN: SMCRA-QA/H1 LIB Radford, VA 24141	1	Assistant Secretary of the Navy (R, E, and S) ATTN: R. Reichenbach Room 5E787 Pentagon Bldg. Washington, DC 20350
1	Commander US Army Foreign Science & Technology Center ATTN: AMXST-MC-3 220 Seventh Street, NE Charlottesville, VA 22901	1	Naval Research Lab Tech Library Washington, DC 20375
2	Commandant US Army Field Artillery Center & School ATTN: ATSF-CO-MW, B. Willis Ft. Sill, OK 73503	2	Commander US Naval Surface Weapons Center ATTN: J. P. Consaga C. Gotzmer Silver Spring, MD 20910
1	Commander US Army Development and Employment Agency ATTN: MODE-TED-SAB Fort Lewis, WA 98433		

# DISTRIBUTION LIST

<u>No. Of Copies</u>	<u>Organization</u>	<u>No. Of Copies</u>	<u>Organization</u>
4	Commander Naval Surface Weapons Center ATTN: S. Jacobs/Code 240 Code 730 K. Kim/Code R-13 R. Bernecker Silver Spring, MD 20910	5	Commander Naval Ordnance Station ATTN: P. L. Stang J. Birkett S. Mitchell D. Brooks Tech Library Indian Head, MD 20640
5	Commander Naval Surface Weapons Center ATTN: Code G33, J. L. East W. Burrell J. Johndrow Code G23, D. McClure Code DX-21 Tech Lib Dahlgren, VA 22448	1	HQ AFSC/SDOA Andrews AFB, MD 20334
2	Commander Naval Underwater Weapons Research and Engineering Station Energy Conversion Dept. ATTN: CODE 5B331, R. S. Lazar Tech Lib Newport, RI 02840	5	AFRPL (DYSC) ATTN: D. George J. N. Levine D. Thrasher N. Vander Hyde Tech Library Edwards AFB, CA 93523
4	Commander Naval Weapons Center ATTN: Code 388, R. L. Derr C. F. Price T. Boggs Info. Sci. Div. China Lake, CA 93555	1	AFFTC ATTN: SSD-Tech Lib Edwards AFB, CA 93523
2	Superintendent Naval Postgraduate School Dept. of Mechanical Engineering Code 1424 Library Monterey, CA 93943	1	AFATL/DLYV Eglin AFB, FL 32542-5000
1	Program Manager AFOSR/(SREP) Directorate of Aerospace Sciences ATTN: L. H. Caveny Bolling AFB, DC 20332	1	AFATL/DLJE Eglin AFB, FL 32542-5000
		1	Air Force Armament Lab. AFATL/DLODL Eglin AFB, FL 32542-5000
		1	AFWL/SUL Kirtland AFB, NM 87117

# DISTRIBUTION LIST

<u>No. Of Copies</u>	<u>Organization</u>	<u>No. Of Copies</u>	<u>Organization</u>
1	Aerodyne Research, Inc. Bedford Research Park ATTN: V. Yousefian Bedford, MA 01730	1	Hercules, Inc Bacchus Works ATTN: K. P. McCarty P. O. Box 98 Magna, UT 84044
1	Aerojet Solid Propulsion Co. ATTN: P. Micheli Sacramento, CA 95813	2	Director Lawrence Livermore National Laboratory ATTN: M. S. L-355, A. Buckingham P. O. Box 808 Livermore, CA 94550
1	Atlantic Research Corporation ATTN: M. K. King 5390 Cheorokee Avenue Alexandria, VA 22314	1	Lawrence Livermore National Laboratory ATTN: M. S. L-355 M. Finger P. O. Box 808 Livermore, CA 94550
1	AVCO Everett Rsch Lab ATTN: D. Stickler 2385 Revere Beach Parkway Everett, MA 02149	1	Olin Corporation Badger Army Ammunition Plant ATTN: R. J. Thiede Baraboo, WI 53913
2	Calspan Corporation ATTN: Tech Library P. O. Box 400 Buffalo, NY 14225	1	Hercules Powder Company Allgheny Ballistics Lab. ATTN: R.B. Miller P.O. Box 210 Cumberland, MD 21501
1	Foster Miller Associates ATTN: A. Erickson 135 Second Avenue Waltham, MA 02154	1	Paul Gough Associates, Inc. ATTN: P. S. Gough P. O. Box 1614, 1048 South St. Portsmouth, NH 03801
1	General Electric Company Armament Systems Dept. ATTN: M. J. Bulman, Room 1311 Lakeside Avenue Burlington, VT 05401	1	Physics International Company ATTN: Library H. Wayne Wampler 2700 Merced Street San Leandro, CA 94577
1	ILTRI ATTN: M. J. Klein 10 W. 35th Street Chicago, IL 60616		

# DISTRIBUTION LIST

<u>No. Of Copies</u>	<u>Organization</u>	<u>No. Of Copies</u>	<u>Organization</u>
2	Rockwell International Rocketdyne Division ATTN: BA08 J. E. Flanagan J. Gray 6633 Canoga Avenue Canoga Park, CA 91304	1	Universal Propulsion Company ATTN: H. J. McSpadden Black Canyon Stage 1 Box 1140 Phoenix, AZ 85029
1	Princeton Combustion Research Lab., Inc. ATTN: M. Summerfield 475 US Highway One Monmouth Junction, NJ 08852	2	United Technologies Chemical Systems Division ATTN: R. Brown Tech Library P. O. Box 358 Sunnyvale, CA 94086
1	Science Applications, Inc. ATTN: R. B. Edelman 23146 Cumorah Crest Woodland Hills, CA 91364	1	Veritay Technology, Inc. 4845 Millersport Hwy. P. O. Box 305 East Amherst, NY 14051-0305
3	Thiokol Corporation Huntsville Division ATTN: D. Flanigan R. Glick Tech Library Huntsville, AL 35807	1	Battelle Memorial Institute ATTN: Tech Library 505 King Avenue Columbus, OH 43201
1	Scientific Research Assoc., Inc. ATTN: H. McDonald P.O. Box 498 Glastonbury, CT 06033	1	Brigham Young University Dept. of Chemical Engineering ATTN: M. Beckstead Provo, UT 84601
1	Thiokol Corporation Wasatch Division ATTN: Tech Library P. O. Box 524 Brigham City, UT 84302	1	California Institute of Tech 204 Karman Lab Main Stop 301-46 ATTN: F. E. C. Culick 1201 E. California Street Pasadena, CA 91109
2	Thiokol Corporation Elkton Division ATTN: R. Biddle Tech Lib. P. O. Box 241 Elkton, MD 21921	1	California Institute of Tech Jet Propulsion Laboratory ATTN: L. D. Strand 4800 Oak Grove Drive Pasadena, CA 91103
		1	Professor Herman Krier Dept of Mech/Indust Engr University of Illinois 144 MEB; 1206 N. Green St. Urbana, IL 61801

# DISTRIBUTION LIST

<u>No. Of</u> <u>Copies</u>	<u>Organization</u>	<u>No. Of</u> <u>Copies</u>	<u>Organization</u>
1	University of Minnesota Dept. of Mechanical Engineering ATTN: E. Fletcher Minneapolis, MN 55455	1	Pennsylvania State University Dept. Of Mechanical Engineering ATTN: K. Kuo University Park, PA 16802
1	University of Massachusetts Dept. of Mechanical Engineering ATTN: K. Jakus Amherst, MA 01002	1	University of Michigan Gas Dynamics Lab./Aerospace Engineering Bldg-G.M. Faeth Ann Arbor, MI 48109-2140
1	Case Western Reserve University Division of Aerospace Sciences ATTN: J. Tien Cleveland, OH 44135	1	Purdue University School of Mechanical Engineering ATTN: J. R. Osborn TSPC Chaffee Hall West Lafayette, IN 47906
3	Georgia Institute of Tech School of Aerospace Eng. ATTN: B. T. Zinn E. Price W. C. Strahle Atlanta, GA 30332	1	SRI International Propulsion Sciences Division ATTN: Tech Library 333 Ravenswood Avenue Menlo Park, CA 94025
1	Institute of Gas Technology ATTN: D. Gidaspow 3424 S. State Street Chicago, IL 60616	1	Rensselaer Polytechnic Inst. Department of Mathematics Troy, NY 12181
1	Johns Hopkins University Applied Physics Laboratory Chemical Propulsion Information Agency ATTN: T. Christian Johns Hopkins Road Laurel, MD 20707	2	Director Los Alamos Scientific Lab ATTN: T3, D. Butler M. Division, B. Craig P. O. Box 1663 Los Alamos, NM 87544
1	Massachusetts Institute of Technology Dept of Mechanical Engineering ATTN: T. Toong 77 Massachusetts Avenue Cambridge, MA 02139	1	Stevens Institute of Technology Davidson Laboratory ATTN: R. McAlevy, III Castle Point Station Hoboken, NJ 07030
		1	Rutgers University Dept. of Mechanical and Aerospace Engineering ATTN: S. Temkin University Heights Campus New Brunswick, NJ 08903

DISTRIBUTION LIST

<u>No. Of Copies</u>	<u>Organization</u>
1	University of Southern California Mechanical Engineering Dept. ATTN: OHE200, M. Gerstein Los Angeles, CA 90007
2	University of Utah Dept. of Chemical Engineering ATTN: A. Baer G. Flandro Salt Lake City, UT 84112
1	Washington State University Dept. of Mechanical Engineering ATTN: C. T. Crowe Pullman, WA 99163

Aberdeen Proving Ground

Dir, USAMSAA  
ATTN: AMXSY-D  
AMXSY-MP, H. Cohen

Cdr, USATECOM  
ATTN: AMSTE-TO-F

Cdr, USACSTA  
ATTN: S. Walton  
G. Rice  
D. Lacey  
C. Herud

Dir, HEL  
ATTN: J. Weisz

Cdr, CRDC, AMCCOM  
ATTN: SMCCR-RSP-A  
SMCCR-MU  
SMCCR-SPS-1L



# USER EVALUATION SHEET/CHANGE OF ADDRESS

This Laboratory undertakes a continuing effort to improve the quality of the reports it publishes. Your comments/answers to the items/questions below will aid us in our efforts.

1. BRL Report Number \_\_\_\_\_ Date of Report \_\_\_\_\_

2. Date Report Received \_\_\_\_\_

3. Does this report satisfy a need? (Comment on purpose, related project, or other area of interest for which the report will be used.) \_\_\_\_\_  
\_\_\_\_\_  
\_\_\_\_\_

4. How specifically, is the report being used? (Information source, design data, procedure, source of ideas, etc.) \_\_\_\_\_  
\_\_\_\_\_  
\_\_\_\_\_

5. Has the information in this report led to any quantitative savings as far as man-hours or dollars saved, operating costs avoided or efficiencies achieved, etc? If so, please elaborate. \_\_\_\_\_  
\_\_\_\_\_  
\_\_\_\_\_

6. General Comments. What do you think should be changed to improve future reports? (Indicate changes to organization, technical content, format, etc.) \_\_\_\_\_  
\_\_\_\_\_  
\_\_\_\_\_

CURRENT  
ADDRESS

Name \_\_\_\_\_  
Organization \_\_\_\_\_  
Address \_\_\_\_\_  
City, State, Zip \_\_\_\_\_

7. If indicating a Change of Address or Address Correction, please provide the New or Correct Address in Block 6 above and the Old or Incorrect address below.

OLD  
ADDRESS

Name \_\_\_\_\_  
Organization \_\_\_\_\_  
Address \_\_\_\_\_  
City, State, Zip \_\_\_\_\_

(Remove this sheet along the perforation, fold as indicated, staple or tape closed, and mail.)